IET Journals
The Institution of Engineering and Technology

ISSN 1751-8644
doi: 0000000000
www.ietdl.org

Personal Verification Based on Multi-Spectral Finger Texture Lighting Images

R. R. O. Al-Nima[1,4], M. T. S. Al-Kaltakchi[2,4], S. A. M. Al-Sumaidaee[3,4], S. S. Dlay[4], W. L. Woo[4], Tingting Han[5], J. A. Chambers[4,6]

[1] *Department of Technical Computer Engineering, Technical College of Mosul, Mosul, Iraq*
[2] *Department of Electrical Engineering, College of Engineering, Al-Mustansiriya University, Baghdad, Iraq*
[3] *Department of Computer and Software Engineering, College of Engineering, Al-Mustansiriya University, Baghdad, Iraq*
[4] *ComS² IP Research Group, School of Electrical and Electronic Engineering, Newcastle University, England, United Kingdom*
[5] *Department of Computer Science and Information Systems, Birkbeck, University of London, London, UK*
[6] *Digital Communications and Intelligent Sensing Research Group, Department of Engineering, University of Leicester, England, United Kingdom*
* *E-mail: m.t.s.al_kaltakchi@uomustnsiriyah.edu.iq,{s.a.m.al-sumaidaee, satnam.dlay, Lok.Woo, Jonathon.Chambers}@ncl.ac.uk*

Abstract: Finger Texture (FT) images acquired from different spectral lighting sensors reveal various features. This inspires the idea of establishing a recognition model between FT features collected using two different spectral lighting forms to provide high recognition performance. This can be implemented by establishing an efficient feature extraction and effective classifier, which can be applied to different FT patterns. So, an effective feature extraction method called the Surrounded Patterns Code (SPC) is adopted. This method can collect the surrounded patterns around the main FT features. It is believed that these patterns are robust and valuable. The SPC approach proposes using a single texture descriptor for FT images captured under multi-spectral illuminations, where this reduces the cost of employing different feature extraction methods for different spectral FT images. Furthermore, a novel classifier termed the Re-enforced Probabilistic Neural Network (RPNN) is proposed. It enhances the capability of the standard Probabilistic Neural Network (PNN) and provides better recognition performance. Two types of FT images from the Multi-Spectral CASIA (MSCASIA) database were employed as two types of spectral sensors were used in the acquiring device: the White (WHT) light and spectral 460 nm of Blue (BLU) light. Supporting comparisons were performed, analysed and discussed. The best results were recorded for the SPC by enhancing the Equal Error Rates (EERs) at 4% for spectral BLU and 2% for spectral WHT. These percentages have been reduced to 0% after utilizing the RPNN.

1 Introduction

The term 'biometric' is currently widely used to indicate an efficient way of recognizing people. It has been explored for many years in different applications. Examples of these applications are security systems, people recognition, and forensic investigations. Many biometric characteristics within the human body have been separately investigated such as the fingerprint [1], iris [2], face [3], palm [4], speaker [5] and Finger Texture (FT) [6]. Furthermore, various studies have also been exploited by utilizing more than one biometric characteristic as in [7].

Rich characteristics can be observed in any single finger. First of all, they hold the most famous biometric, which is the fingerprint, in addition to other attractive biometrics such as Finger Geometry (FG), Finger Veins (FV), Finger Outer Knuckle (FOK), Finger Inner Knuckle (FIK) and Finger Texture (FT).

Inner finger surface texture has drawn considerable attention over approximately the last ten years and it has similar patterns to the palm. These patterns are known as the FT, and they mainly include wrinkles and principal lines. FTs are reliable and unique between the individuals and even between the identical twins [8]. Furthermore, there are many advantages beyond using the FTs such as they involve rich information, they resist to emotional feelings, and their patterns are stable and reliable [8]. They can be found on the inner surface of the index, middle, ring and little fingers. Principally, the FT is positioned between the upper phalanx (directly under the fingerprint) and the lower knuckle (the base of the finger). It comprises of three phalanxes and three knuckles. Thus, it involves different qualified patterns. The main FT locations in a hand image are given in Fig. 1(a), whereas, the main FT parts in a single finger are given in Fig. 1(b).

It has been cited that using one sensor to acquire a single type of biometric features can cause series verification obstacles [9]. In addition, it has been confirmed that by applying different spectral lightings during the acquisition step, various FT features are revealed [10]. This has inspired the idea of this paper. So, the aim of this study is to suggest a powerful human verification system based on multi-spectral FT features.

The contributions of this work are as follows:

- Establishing a new feature extraction method called the Surrounded Patterns Code (SPC) robust to collect the surrounded patterns around the main FT features, which acquired under multi-spectral illuminations.
- Designing and implementing a novel neural network called the Re-enforced Probabilistic Neural Network (RPNN), which intends to contribute to this growing area of recognition research.

Different comparisons are performed to demonstrate the ability and efficiency of the proposed methods. The results are provided by employing FT images of two spectra that collected from the MSCASIA Palmprint image database (Version 1.0) [11].

This paper is organised as follows: Section 2 states the prior work, Section 3 illustrates the methodology of the suggested SPC, Section 4 describes the architecture of the proposed RPNN, Section 5 discusses the obtained results and Section 6 concludes this paper.

2 Prior work

The idea of employing the FTs probably started by Ribaric and Fratric [12], where this study introduced a multi-modal biometric system by using eigenfinger and eigenpalm features. In this publication a scanner device was used to acquire high resolution hand

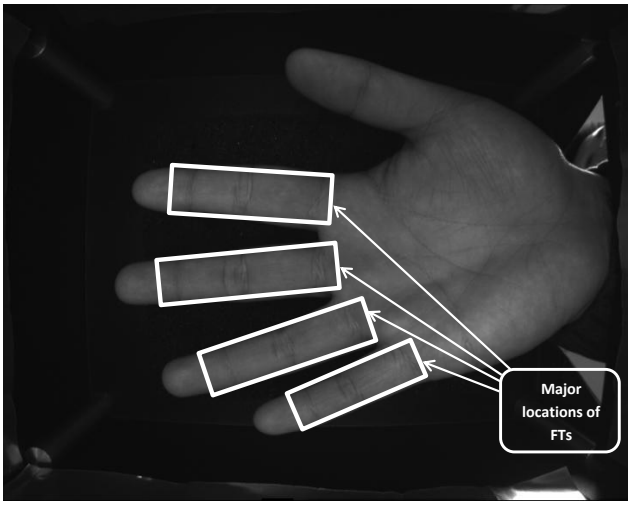

(a)

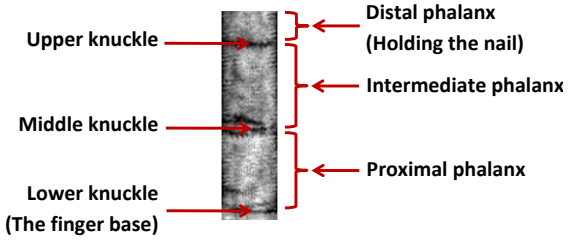

(b)

Fig. 1: The main positions and parts of the FTs:
a The main positions of the FTs, they are distributed in the inner surface of fingers. They are located between the upper phalanx (under the fingerprint) and the lower knuckle (the base of the finger)
b The main FT parts in a single finger. It consists of three phalanxes (distal, intermediate and proximal) and three knuckles (upper, middle and lower)

images. So, the hands of the participants were located in a specific position with small limitations for finger translations. In this study a fixed ratio size of the FT is considered in each finger. This means that not all the FT regions were covered because the fingers have different sizes. Pavesic *et al.* [13] established a study to fuse the fingerprints with the FTs for each finger. The authors also used a scanner acquisition device to collect part of hand images. So, they used high resolution part hand images located in a limited space, which allowed just small finger movements. The thumb was excluded with parts of upper and lower knuckles of the four fingers (index, middle, ring and little). Furthermore, the authors assigned for each finger a fixed ratio size of the FT region, which may cause parts of the finger width to be cancelled. Michael *et al.* [14, 15] designed a system to track hand fingers from a video stream. A web camera and warm-white light bulb were utilized. Furthermore, a fusion method between the FTs and the palm print was presented. A score fusion was exploited, but by applying the Support Vector Machine (SVM) technique with the kernel of Radial Basis Function (RBF). Before that, a matching was applied by using the Hamming distance for the palm print and Euclidean distance for the FTs. Kanhangad *et al.* [16] established combination work of various hand characteristics. Basically, these characteristics were FTs; hand geometry and palm print. Furthermore, 2D and 3D biometric features were studied for the hand geometry and palm print. A database called the Hong Kong Polytechnic University Contact-free 3D/2D (PolyU3D2D) Hand Images Database (Version 1.0) [17] was used. The hand images of this database were collected under normal lighting. Zhang *et al.* [18] utilized the features of the middle finger and the palm print in a Single Sample Biometrics Recognition (SSBR), where both can be acquired from a single image. Part of the lower knuckle is included. It can be investigated that low resolution FT images of 30×90 pixels were collected. So, it is not worth to include the fingerprint with the FT, because the fingerprint patterns cannot be involved. Sankaran *et al.* [19] described a finger-photo verification by using the mobile phone camera. In this paper, the FT is used with the fingerprint. Only two right hand fingers were employed, the middle and index fingers. Furthermore, a part of the lower FT area was not covered (the proximal phalanx with the lower knuckle or sometimes only the lower knuckle). So, this study was not comprehensively established for the FTs.

-Al-Nima *et al.* [20] proposed a method to extract the full regions of the FTs from the four fingers based on the traditional contour. This publication confirmed that increasing the collected FT patterns would increase the performance of the biometric recognition. Effectively, the main FT regions for the four fingers were assigned in this study. The PolyU3D2D database was used, as mentioned the images of this database are acquired under a normal lighting. Al-Nima *et al.* [10, 21, 22] employed feature level fusion based on the concatenation rule between the FT features of fingers. More experiments were included in [10] to examine the verification performance with missing finger elements (or parts). For example, removing a distal phalanx; a distal and an intermediate phalanxes; one finger and two fingers. An approach has also been suggested, implemented and analysed to increase the verification performance rates in the case of such missing elements. Additional combination method was explained in [22], where a novel neural network named the Finger Contribution Fusion Neural Network (FCFNN) has been suggested. The FCFNN fuses the contribution scores of the finger objects. This approach was inspired from the different contribution of each finger, where the contribution score of any finger in terms of individual verification is not the same as the contribution score of the another finger. Different databases were utilized by [10, 21, 22] in which a single lighting source is exploited.

It can be investigated from the previous literature that no study has considered employing different FT features acquired from different lighting sensors. The specifications of the MSCASIA database have been found to be valuable in this paper. By using various FT specifications captured from different spectra, an efficient personal biometric recognition system can be established.

3 The Feature Extraction Approach

A segmentation approach that was suggested in [10] to isolate finger areas from contact-free hand images is employed in this study. It consists of several image processing steps which were designed to maintain the hand area and detect the fingers. These steps are collecting the grayscale hand image; applying a binarization operation; removing all the small noises around the largest hand region; complementing the resulting image; deleting the noises which might exist within the hand border and detecting the finger objects. Henceforth, the main finger points (tip, valley and symmetric) can be determined and used to segment the finger images. Then, segmenting the four finger images of (little, ring, middle and index) are carried out. It is worth mentioning that additional pixels have been included with each segmented finger image to cover the patterns of the lower knuckles as these patterns can enhance the verification performance according to [20].

After that, extracting the Region of Interest (ROI) of the FT has been performed. A useful method has been utilized based on the adaptive inner rectangle. This method has been reported in [16], where an adaptive inner rectangle was applied to extract the ROI for the four fingers. In this publication the lower or third inner knuckle was not considered and thus important features of the FTs are avoided. A further modified model for the adaptive ROI rectangle is applied here, where the lower knuckles are collected for each finger. After specifying the ROI, fixed resizing has been applied.

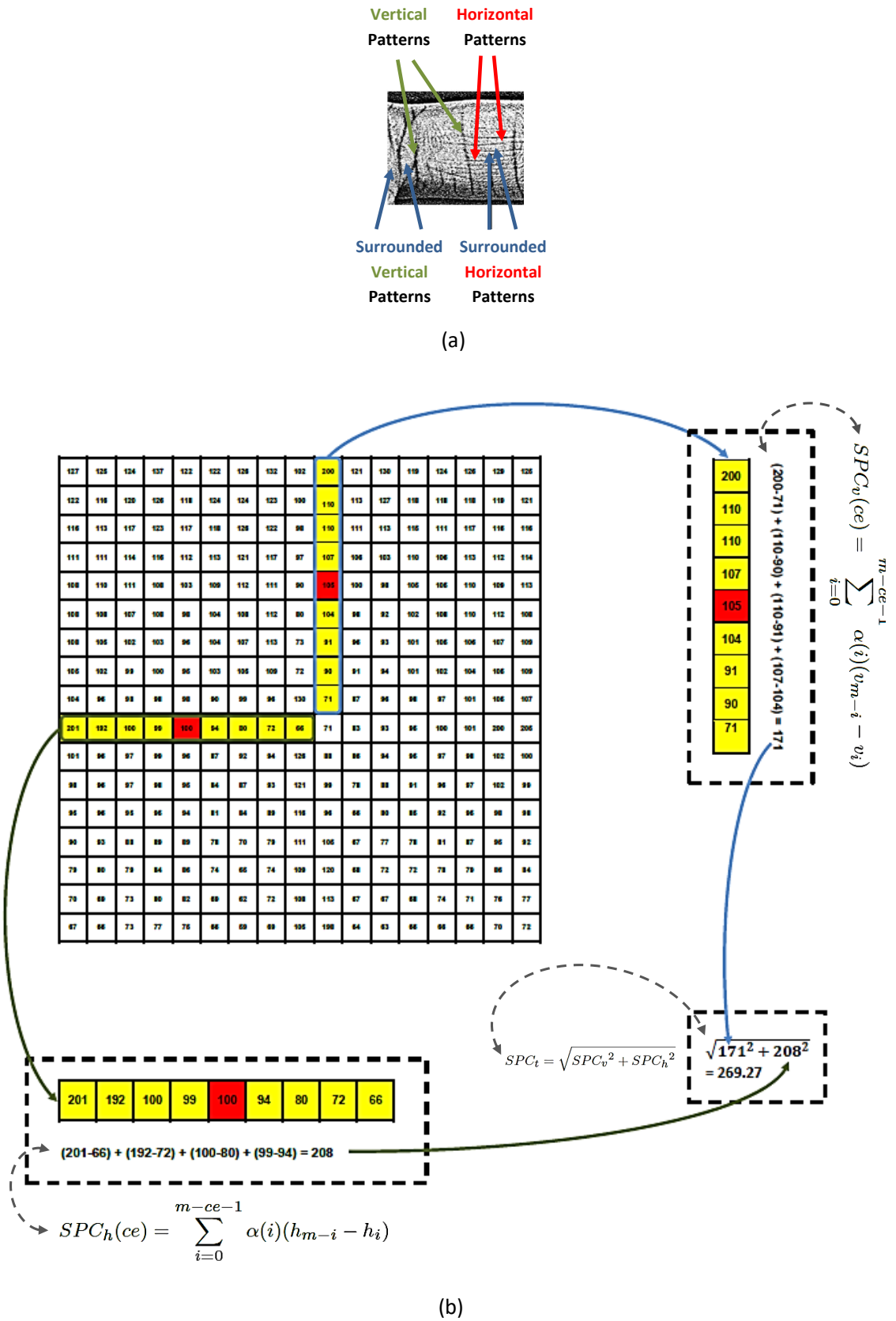

Fig. 2: Demonstrating the SPC feature extraction method:
a Locations of surrounded patterns, they surround the horizontal and vertical patterns
b Example of analysing the vertical and horizontal patterns by using the SPC

IET Research Journals, pp. 1–10

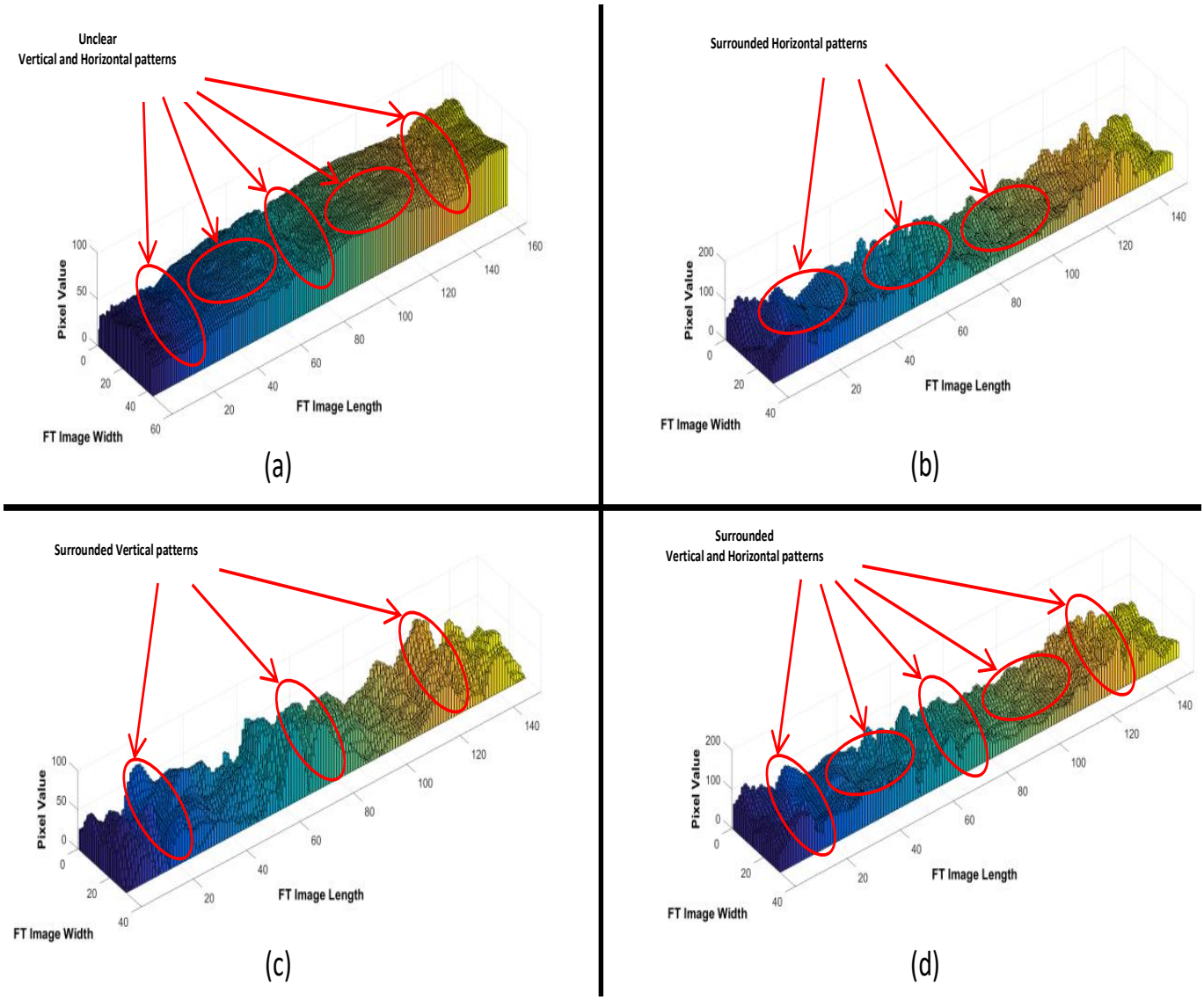

Fig. 3: 3D bar analysis for a BLU spectral FT image of a middle finger. (a) Pixel levels of the original FT image. (b) Pixel levels of the horizontal patterns. (c) Pixel levels of the vertical patterns. (d) Pixel levels of the fusion between the vertical and horizontal patterns.

The normalization resize is considered equal to 30×150 following [6, 10, 21, 22].

Hereafter, a new feature extraction approach to analyse the FT features of different spectra, specifically the BLU and WHT, is adopted. The feature extraction is performed to each ROI image by using the SPC method. Then, the Coefficient of Variance (COV) calculations is used following [6, 10, 20]. The resulted COV values have been used as inputs to the RPNN.

SPC feature extraction can effectively analyse the vertical and horizontal patterns of FTs. The output of the SPC is an enhanced image, which is resulted after applying the SPC calculations.

First of all, differences between symmetric pixels of vertical and horizontal vectors are separately calculated according to the following equations:

$$SPC_v(ce) = \sum_{i=0}^{m-ce-1} \alpha(i)(v_{m-i} - v_i) \quad (1)$$

$$SPC_h(ce) = \sum_{i=0}^{m-ce-1} \alpha(i)(h_{m-i} - h_i) \quad (2)$$

where: SPC_v is the extracted value from the vertical vector, SPC_h is the extracted value from the horizontal vector, ce is the location of the centre pixel in either the vertical or the horizontal vector and it is equal to $\lceil \frac{m}{2} \rceil$ where $\lceil . \rceil$ represents the ceiling operator, $\alpha(i)$ is the sign of the subtraction operation, m is the vector length, v is the vertical pixels along the vertical vector, and h is the horizontal pixels along the horizontal vector.

This idea is similar to the difference filter. Nevertheless, the difference filter considers the differences between only two neighbour values and this is not sufficient to clarify the surrounded patterns.

Hence, two main possibilities can be achieved. Firstly, the horizontal or vertical code has a low or zero value, this is resulting from the differences between two half vectors, which have almost equalized symmetric pixel values. Secondly, the horizontal or vertical code has high absolute value, this is resulting from two significant differences between symmetric pixel values around the horizontal or vertical vector. The second possibility can enhance the contrast of the surrounded patterns.

Basically, the $SPC_v(ce)$ is assigned to analyse the FT vertical patterns. Whereas, the $SPC_h(ce)$ is determined to analyse the horizontal FT patterns. Consequently, the amplitude equation is used to obtain the desired code of the SPC according to the following equation:

$$SPC_t = \sqrt{{SPC_v}^2 + {SPC_h}^2} \quad (3)$$

where: SPC_t is the magnitude code between the resulted values of the vertical and horizontal filters. Figs. 2(a and b) demonstrates the SPC locations and operations.

This suggested feature extraction has the following utilities: it calculates single-dimensional filters for each of the two directions (vertical and horizontal); it considers the differences between symmetric pixel values around the centre pixels of vertical or horizontal vectors; and it adaptively adjusts the difference sign value α between {1,-1} according to the subtraction operation. In addition, the SPC operator does not involve many operations as in [23].

After applying the SPC feature extraction approach to both WHT and BLU spectra FT images, it has been resulted that the surrounded features were efficiently described. To illustrate, both the surrounded horizontal and vertical FT patterns have been extracted and the new form of the FT has been found to be more robust in terms of describing these features. An example of 3D bar plots of the distributed FT pixels prior to, during and after the SPC are given in Fig. 3.

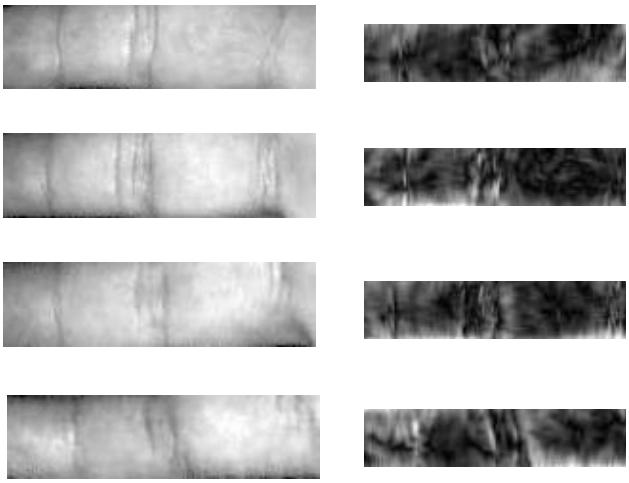

Fig. 4: FT images of the WHT spectral before and after the SPC. The first column in the left is for the original FT images. The second column in the right is for the SPC images. Additionally, the rows are assigned for the four fingers, from the top index; middle; ring and little fingers, respectively.

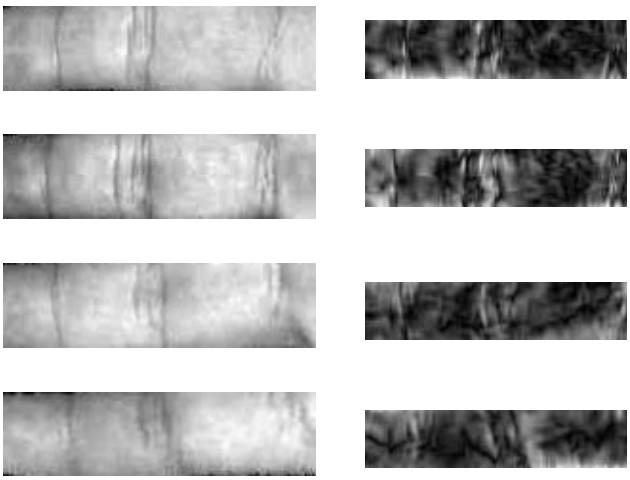

Fig. 5: FT images of the BLU spectral before and after the SPC. The first column in the left is for the original FT images. The second column in the right is for the SPC images. Additionally, the rows are assigned for the four fingers, from the top index; middle; ring and little fingers, respectively.

From this figure, it can be seen that the distribution of FT pixel values before using the SPC operation were smoothly flows. In other words, the contrast between the FT features was not clear. After calculating the SPC_v values, the surrounded horizontal patterns of the FT are extracted. Likewise, after computing the SPC_h values, the surrounded vertical patterns of the FT are collected. Subsequently, combining the extracted vertical and horizontal features by calculating the SPC_t values caused the surrounded patterns to be efficiently described. That is, clear contrasted FT images are constructed, where the surrounded FT patterns can be recognized.

Moreover, Figs. 4 and 5 reveals that various patterns can be extracted from the different fingers. Furthermore, various features can be collected after employing different spectral lightings. This fact was also confirmed in [24] and [10].

To calculate the COV values, each SPC image is partitioned into non-overlapped windows. The COV value of each window can be calculated according to the following equations [25]:

$$M_{seg} = \frac{1}{n}\sum_{i=1}^{n} seg_i \tag{4}$$

$$STD_{seg} = \sqrt{\frac{1}{n-1}\sum_{i=1}^{n}(seg_i - Mseg)^2} \tag{5}$$

$$COV_{seg} = \frac{STD_{seg}}{M_{seg}} \tag{6}$$

where n is the number of pixels in each window, seg is a 5×5 pixels window just as in [6, 10, 20], M is the mean, STD is the standard deviation and COV is the coefficient of variance value.

The COV has the following advantages: it reduces the image size, where each image window has been reduced to one value; it is easy to calculate; it efficiently describes the variances between the pixel values [10]; all values are small and positive; the variances between the features for the same subject are well described and the variances between the features for different subjects are well described [6].

4 The Re-enforced Probabilistic Neural Network

In this context, a novel RPNN is proposed for verification. Fundamentally, the computations of this network are motivated from the PNN. However, the standard PNN works in a feedforward policy and it calculates the probabilities of the most corresponding weights to specific input values. Therefore, if the extracted feature values of the certain input are not accurate, the PNN will generate incorrect verification decision. Also, its output decision affects by the quality and accuracy of the provided input. From this point, the RPNN can overcome this drawback by considering a feedback from the output to the hidden layer and allowing supported input and weight values to be carried out by the network. In this case the verification performance can be further enhanced.

The proposed RPNN consists of input layer; hidden layer; summation layer and decision layer. Furthermore, connection weights are distributed between the layers just as the PNN. However, feedback connection weights are considered between the output layer and the hidden layer. Fig. 6 demonstrates the structure of the suggested RPNN.

The RPNN operations can be explained as follows: the hidden values of the hidden layer are calculated according to Equation (7) [26], this equation is also known as the Radial Basis Function (RBF):

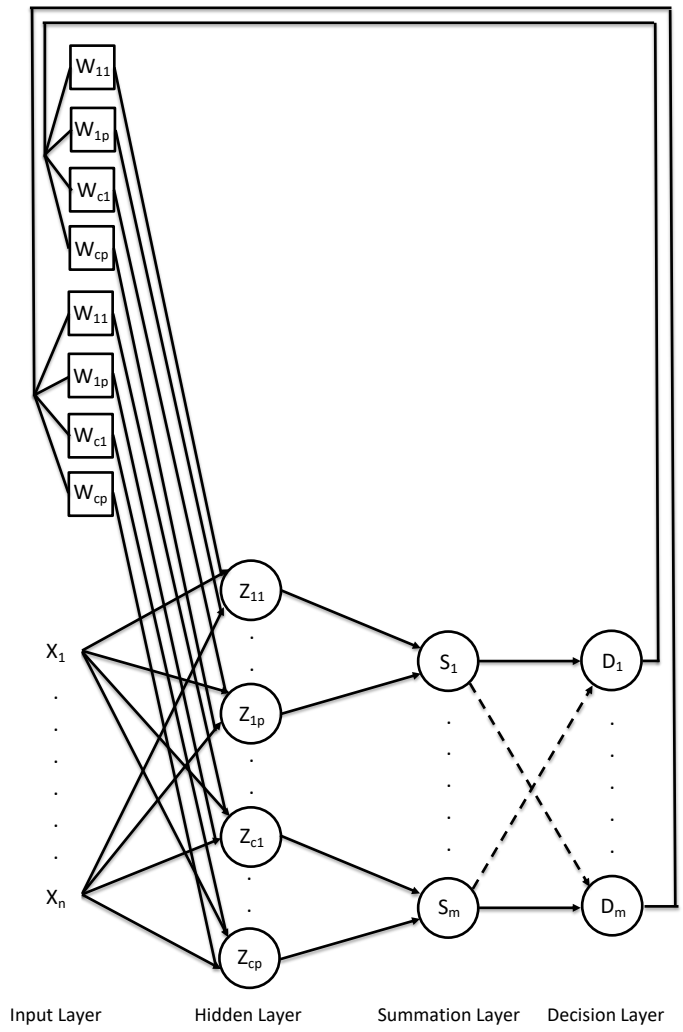

Fig. 6: The general architecture of the RPNN composes of an input layer; hidden layer; summation layer; decision layer and feedback.

$$Z_{i,j} = exp\left[-\frac{(\mathbf{x}^{\lambda} - \mathbf{w}_{i,j}^{\lambda})^T(\mathbf{x}^{\lambda} - \mathbf{w}_{i,j}^{\lambda})}{2\sigma^2}\right], \quad i = 1, 2, ..., p\ ,\ j = 1, 2, ..., c \tag{7}$$

where $Z_{i,j}$ represents a hidden layer node value, $\mathbf{x}^{\lambda}$ represents the input vector $\mathbf{x}^{\lambda} = [x_1^{\lambda}, x_2^{\lambda}, ..., x_n^{\lambda}]^T$, $\mathbf{w}_{i,j}^{\lambda}$ is the i^{th} vector of class j, thus, the weight vector can be described or formed as $\mathbf{w}_{i,j}^{\lambda} = [w_1^{\lambda}, w_2^{\lambda}, ..., w_n^{\lambda}]^T$, λ represents the certain spectral {1,2}, σ is the spread controlling parameter of the Gaussian function, p is the number of the training vectors in each class and c is the number of classes or subjects.

The summation layer will collect the hidden values from the hidden layer and assign the trained input vectors to specific classes:

$$S_j = \frac{1}{p}\sum_{i=1}^{p} Z_{i,j}, \quad j = 1, 2, ..., c \tag{8}$$

where S_j is a summation layer node value.

The decision layer will perform a winner takes all rule by utilizing the following Equation (9):

$$D_j = \begin{cases} 1 & \text{if } S_j = max \\ 0 & \text{otherwise} \end{cases}, \quad j = 1, 2, ..., c \tag{9}$$

where D_j is a decision layer node value and max is the maximum S_j value.

Basically, the RPNN aims to generate weight values in the training phase to establish a non-linear relationship between the inputs and targets. Then, these weights can be saved in a template file and used in the testing phase to predict the outputs according to the provided inputs. In the training phase (or registration step), the weight values are generated exactly equal to the training input values. The RPNN stores the main weights (or the training inputs of spectral BLU) between the input and hidden layers, whereas, the RPNN saves the supported weights (or the training inputs of spectral WHT) between the output and hidden layers. The COV values of the FTs of four fingers (index, middle, ring and little) are concatenated and used as inputs to the RPNN, overall 720 input values for each sample. Whilst, each node in the output of the RPNN refers to a subject or person. So, 100 nodes have been used for the RPNN, where these are exactly equal to the number of people who provided their images in the database. The output decision values are set as logic '1' for the determined subject or person and '0's to all other nodes.

In the training phase, the RPNN stores the $\mathbf{w}_{i,j}^{\lambda}$ weights. The main weights will be saved between the input and hidden layers, whereas, the supported weights will be saved between the output and hidden layers. In the testing phase, all the above mentioned equations are considered, but for new hand images. Hence, if the claimed verification for a certain subject or class is not correct, the λ will be changed to the second supported features from the second spectral and its feedback weights will be used instead of the forward weights. In this case, the second spectral inputs $\mathbf{x}^{\lambda}$ will be given. The first inputs have been chosen for the BLU features following [10, 22], so, the supported FT features belong to the WHT. The last step is to obtain the final verification decision.

There are some interesting points which can be highlighted for the RPNN: it is not affected by the local minimum error in the cost function; the training phase is very fast as it requires only one iteration to complete all the training and two iterations to complete the testing part; it has the ability to include additional users; it has the ability to delete trained users and it provides measures of confidences by considering the probabilities of the inputs.

It is true that the network requires reasonable size of memory. However, this is not a big issue because of the availability of computers with large memories. It is believed that the high verification accuracy, which can be provided by the RPNN, is more important than the required size of the memory. Furthermore, the featured vectors have much reduced sizes than the original images of the fingers.

5 RESULTS AND DISCUSSIONS

5.1 Applied Database

With the CASIA Multi-Spectral Palmprint Image Database (Version 1.0), or simply MSCASIA database, multi-spectral light sensors were used to capture different features of the hand images. Principally, the skin of an inner hand surface appears various characteristics if different spectral lightings are applied. This is due to the penetration of the given spectral. A multi-spectral acquisition device was established to capture six patterns types of hand images. These images have been made open access to expand the studies of biometrics. It is touchless as there are no limitations to the location of the hand. However, the participants were expected to open their hands inside the acquisition box. A dark background (mainly black) was used. A Charge Coupled Device (CCD) camera was located at the bottom of the device and the lighting was equally distributed. A total of 100 users contributed with their right and left hand images. Six samples were captured in two sessions. That is, three samples

were captured in session one and after just over a month, in session two, an additional three samples were collected. Multi-spectral lightings were used to capture six image patterns at a certain time. The utilized spectra had the illuminations of 460 nm, 630 nm, 700 nm, 850 nm, 940 nm and WHT. Therefore, the total number of provided MSCASIA images in this database was 7,200 right and left hand images. They were stored as JPEG images and they are all of 8-bits grayscale. In the case of resolution, each hand image had 576×768 pixels [11]. Basically, the wavelengths of 630 nm and 850 nm contains FTs with veins, and the wavelengths of 700 nm and 850 nm contains only veins. In this study, hand images of spectral 460 nm are employed, because spectral wavelength BLU contains only the FTs as stated in [27, 28]. In addition, hand images that acquired by using the WHT light sensor also provide FT patterns, due to the fact that only the FTs can be seen under the normal visible light. It is thus a good opportunity to study the specifications of the FTs under different spectral lights.

Four fingers (the index, middle, ring and little fingers) from the right hand images for both employed spectra were segmented according to [10]. A total of 4,800 finger images are used in this study, 2,400 finger images for spectral WHT, and the rest of finger images are used for spectral BLU of the same database. For the training phase, 4,000 fingers have been exploited, and for the testing phase, 800 fingers have been utilized. It is true that the number of testing samples was small, but this is the same number of training samples in [6, 10, 16, 20]. This will allow fair justifications with the state-of-the-art work. Nevertheless, additional experiments have been applied by varying the number of training/testing samples and recording the obtained EERs.

5.2 Results and Discussions for the SPC

First of all, the SPC has been implemented to each FT as demonstrated in Figs. 2, 3, 4 and 5. To illustrate, the surrounded vertical and horizontal patterns, which are located around the main FT patterns as shown in Fig. 2(a), of each FT image have been analysed as represented in Fig. 2(b) by applying the SPC calculations according to Equations (1), (2) and (3). Principally, the original FT image shows low contrast levels to overall information as presented in Fig. 3(a). After analysing the surrounded horizontal patterns, high contrast levels are clarified between them as shown in Fig. 3(b). Likewise, after analysing the surrounded vertical patterns, high contrast levels are constructed between them as shown in Fig. 3(c). By combining both contrasted patterns, rich and effective levels of information are resulted as presented in Fig. 3(d). So, the resulted images show high contrast information between the surrounded patterns as the given examples in Figs. 4 and 5 for WHT and BLU spectral images respectively, where groups of FT images are demonstrated before and after the SPC feature extraction.

Both FT spectra were evaluated with the SPC feature extraction. The first important examination to be considered is the length of the vertical or horizontal vector N (in pixels) as different lengths provide various pattern scales. So, the most appropriate patterns were investigated for each spectral with the standard PNN in terms of obtaining the best EER value. Figs. 7(a) and 7(b) show results of various SPC lengths for both the WHT and BLU databases, respectively. It is clear from Fig. 7(a) that N = 9 has achieved the best EER for the WHT features compared with other lengths as increasing or decreasing the number of pixels would change the effectiveness of the resulted SPC patterns. In Fig. 7(b), several number of lengths has attained the best reported EER for the BLU features, these are N = 11, N = 13, N = 15 and N = 17. Therefore, to select the best length additional evaluation has been applied. That is, the time consuming of applying the SPC function to each of the certain length. Fig. 7(c) indicates that reducing the number of processed pixels will decrease the required processing time. So, choosing the smallest length which can attain the least EER value is preferable. Thus, the length of N = 11 has been selected for the SPC in the BLU database, because this length recorded faster time than the lengths of N = 13, N = 15 and N = 17.

Table 1 shows comparisons between the various types of feature extraction approaches by using the standard PNN. It can be seen

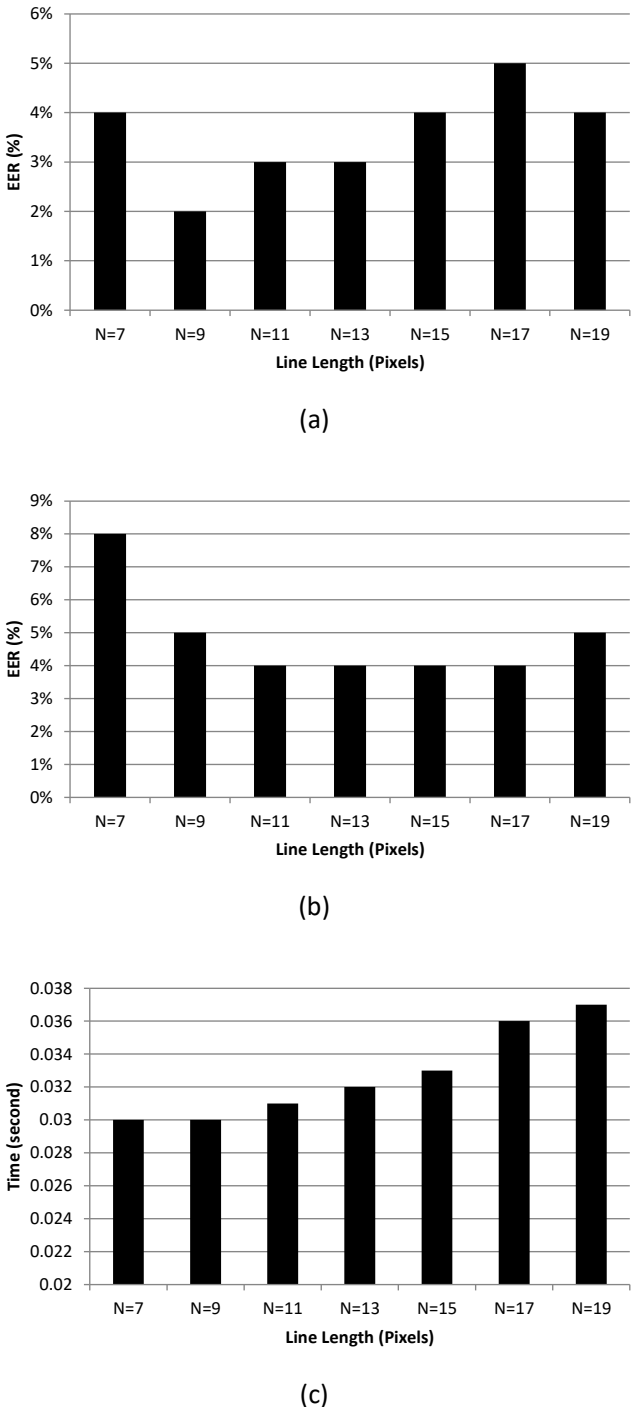

Fig. 7: Examining the length of the SPC vectors:
a SPC vectors lengths versus EER performances for the WHT database
b SPC vectors lengths versus EER performances for the BLU database
c SPC vectors lengths versus timings

from this table that inferior EER values of 60% and 78% have been reported for the method, which is the Centralized Binary Patterns (CBP), that calculates the diagonals patterns and perform fewer computations to all directions (both diagonals, horizontal and vertical). The Local Gradient Coding-Horizontal and Diagonal (LGC-HD) method attained high EER values of 22% and 27% because it computes the gradients of the diagonal patterns and the gradients of the horizontal patterns. However, it ignores the calculations of the vertical patterns, which are very important for FTs. Both the Three-Patch LBP (TPLBP) and the Simplified LBP (SLBP) recorded comparable performance 13% and 12% respectively for the FTs of the WHT

Table 1 Results of different feature extraction methods for the FTs of the four fingers by using the standard PNN

CASIA database (spectral WHT)			
Reference	Method	Parameters	EER
[29]	CBP	Neighbourhood Pixels=8, Radius=2	60%
[30]	LGC-HD	Neighbourhood Pixels=8, Radius=1	22%
[31]	TPLBP	Patch size=3, Radius=2, No. of patches=8, Step jump=5 and Threshold=0.01	13%
[32]	SLBP	Neighbourhood Pixels=8, Radius=1	12%
[20]	IFE	Exponential histogram	10%
[10]	ELLBP	Vertical patterns weight=0.7 and horizontal patterns weight=0.3	7%
[22]	MSALBP	Neighbourhood Pixels=8, Radius=2	5%
Proposed approach	SPC	—	**2%**
CASIA database (spectral BLU)			
Reference	Method	Parameters	EER
[29]	CBP	Neighbourhood Pixels=8, Radius=2	78%
[30]	LGC-HD	Neighbourhood Pixels=8, Radius=1	27%
[31]	TPLBP	Patch size=3, Radius=2, No. of patches=8, Step jump=5 and Threshold=0.01	34%
[32]	SLBP	Neighbourhood Pixels=8, Radius=1	32%
[20]	IFE	Exponential histogram	11%
[10]	ELLBP	Vertical patterns weight=0.2 and horizontal patterns weight=0.8	5%
[22]	MSALBP	Neighbourhood Pixels=8, Radius=2	5%
Proposed approach	SPC	—	**4%**

spectral, but low comparable performance 34% and 32% respectively for the FTs of the BLU spectral. This is because they consider clear textures which can be collected from normal lighting, but they have low performance for the micro-textures obtained from the low wavelength lighting. The novel feature extraction approach, which is termed the Image Feature Enhancement (IFE) has achieved slightly high EER values of 7% and 11% for the WHT and BLU spectra, respectively. This is due to the key idea of this method, where it aimed to enhance the contrast between the top and bottom values of the image features in general. On the other hand, the ELLBP method recorded reasonable EER values of 7% and 5% for the WHT and BLU spectra respectively as this method has the ability of efficiently analyse the FT features. That is, the ELLBP concentrates on the vertical and horizontal patterns, and obviously these are the main patterns of the FT. Also, it efficiently calculates their weights in its weighted summation equation. The best ELLBP parameters for spectral BLU have been found to be $v_1 = 0.2$ and $v_2 = 0.8$ [10]. However, the effective FT parameters for the WHT light have empirically been investigated to be $v_1 = 0.7$ and $v_2 = 0.3$. It is worth mentioning that these are exactly the same parameter values of the Indian Institute of Technology (IIT) Delhi database in [10] as the images of this database were collected under normal lighting. The MASLBP can be considered as one of the most recent and effective FT feature extraction approaches. It obtained comparable results with the ELLBP feature extraction, 5% in both the WHT and BLU spectra of the MSCASIA database. This is because that the MSALBP also focuses on the main FT patterns of the vertical and horizontal. Clearly, the proposed SPC feature extraction attained best verification performances of 2% and 4% for both the WHT and BLU spectra respectively, which means that this method can provide best descriptions for multi-spectral FT patterns.

To summarize, the advantages of the SPC feature extraction are as follows:
1. It is robust to collect the surrounded patterns around the main FT features.
2. It is simple to implement and it can be used with different spectra of FT images. So, this will reduce the cost of utilizing different feature extraction algorithms to analyse the different spectral images.
3. It can obtain better verification accuracy than other Feature extraction methods, as shown in Table 1.

5.3 Results and Discussions for the RPNN

The FT images have been divided for each individual into two parts; the first part is used in the training phase and the second part in the testing phase. This will ensure that the neural network will test new FT images which have not been given before.

During the training phase, the RPNN has been trained for each subject by the input values of spectral BLU and spectral WHT. The first inputs have been chosen for the BLU features following [10, 22] and the supported inputs have been selected for the WHT. Due to the fact that the RPNN saves the input values (as the PNN), the main weights (from BLU) have been saved between the input and hidden layers and the supported weights (from WHT) have been saved between the output and hidden layers. During the testing phase, new FT images have been considered. The input values of the BLU spectral have been examined by the RPNN in a forward direction. Hence, when the claimed verification of a certain subject was not correct, the RPNN was switched to the supported values of the second spectral. So, its feedback weights have been employed instead of the forward weights and the COV values of the WHT spectral have been used in the input. Finally, the verification results have been recorded.

A novel approach that has been suggested in [6] is utilized in this paper to generate the Receiver Operating Characteristic (ROC) graph from the RPNN. Fig. 8(a) illustrates three ROC curves, two curves for the two spectral databases after employing the standard PNN and another curve after applying the RPNN. This is the first time that the ROC curve is produced for the RPNN. To establish the ROC

Table 2 Review summary of the prior work for the four fingers without and with the lower knuckles

Reference	Feature extraction method	Employed classifier	Database	EER (Without the inner knuckles)	EER (With the inner knuckles)
[16]	CompCode	HD	PolyU3D2D	6%	—
[20]	IFE based flat histogram	PNN	PolyU3D2D	5.54%	4.07%
	IFE based exponential histogram	PNN	PolyU3D2D	5.42%	4.07%
	IFE based bell-shaped histogram	PNN	PolyU3D2D	12.66%	7.01%
[6]	LBP	PNN	PolyU3D2D	1.81%	—
	Gabor	PNN	PolyU3D2D	4.97%	—
	—	PNN	PolyU3D2D	16.95%	—
[10]	ELLBP	PNN	PolyU3D2D	0.68%	0.45%
		PNN	IIT Delhi	—	3.38%
		PNN	MSCASIA (Spectral BLU)	—	5%
[22]	MSALBP	PNN	PolyU3D2D	—	0.79%
		FCFNN	PolyU3D2D	—	0.34%
		PNN	MSCASIA (Spectral BLU)	—	5%
		FCFNN	MSCASIA (Spectral BLU)	—	2%
This work	SPC	RPNN	MSCASIA (Spectral BLU and Spectral WHT)	—	**0%**

curve for the RPNN the following steps can be followed: collecting the score values from the summation layer; remapping their values according to the desired targets; extracting the False Acceptance Rate (FAR) and True Positive Rate (TPR) values for each class; calculating the averages of FARs and TPRs for all classes; and depicting the ROC curve. These steps were inspired from [6] and have been applied to the RPNN as first time in this paper.

With the state-of-the-art, Table 2 summarises previous FT studies and the current approaches. The majority of these studies such as [6, 16, 20] have employed the PolyU3D2D Database [17]. This database has 1,770 hand images, each participant provided his/her hand images to be acquired from a distance of approximately 0.7 metres. The major problem with this database is that it includes very low resolution images. Kanhangad *et al.* used this database in [16], where series of operations were adopted: segmenting the finger images; extracting the ROIs; using the CompCode feature analysis method and applying the Hamming Distance (HD) to measure the variances between the samples. A high EER value was recorded to 6% and this is due to the suggested finger segmentations and ROI extraction methods, where the lower knuckles of the FTs were completely ignored. In [20], it was confirmed that the lower knuckles have important features as after including these patterns improvements were recorded in the recognition performance using three different feature analysis methods. The authors adopted a novel feature enhancement approach called the IFE, which consists of multiple processes starting from the Contrast Limited Adaptive Histogram Equalization (CLAHE) and increasing the contrast between the highest values and the lowest values of the FT images. Three types of CLAHE histograms were examined: flat, exponential and bell-shaped histograms, they attained 5.54%, 5.42% and 12.66%, respectively for FTs without the inner knuckles, and they achieved 4.07%, 4.07% and 7.01%, respectively for FTs with the inner knuckles. The worst result was for the IFE based bell-shaped histogram. A new approach was presented in [6] to establish a Receiver Operating Characteristic (ROC) graph for a multiple class PNN. Three feature analysis methods were employed to clarify the ability of the proposed approach: the Local Binary Patterns (LBP), the Gabor filter and using the FTs images without analysis, they obtained 1.81%, 4.97% and 16.95%, respectively. It can be investigated that all the presented state-of-the-art processes applied COV statistical measurements, except [16]. It appears that this strategy has effective computations for determining the variances between the data. A detailed study of using the FTs for the personal verification was introduced in [10]. This study has different contributions. Three hand image databases were employed: the PolyU3D2D [17], IIT Delhi [33, 34] and spectral 460 from the MSCASIA [11]. ELLBP feature extraction approach was applied to these databases and recorded low EER percentages of 0.45%, 3.38% and 5%, respectively. Extended FT study was presented in [22], it presented two new approaches: the MSALBP feature extraction and the FCFNN fusion classifier. It can be seen that the results were further enhanced after using both approaches together, from 0.79% to 0.34% and from 5% to 2% for the PolyU3D2D and MSCASIA (spectral BLU), respectively. Finally, in this paper the SPC method and RPNN is adopted with the two MSCASIA databases (images of spectral BLU and images of spectral WHT). The proposed SPC and RPNN provide superior benchmarked performance over various feature extractions and classifiers in previous work. The best verification performance has been benchmarked to EER=0%. Basically, the EER value for spectral BLU was 4% and the EER value for spectral WHT was 2%.

Finally, all the previous work has employed 5 training and 1 testing samples for a hand fingers of each individual. Obviously, the number of training samples are too big comparing with the number of testing samples. Therefore, additional experiments have been established by reducing the number of the training samples of hand fingers and increasing the number of the testing samples of the same hand fingers. Fig. 8(b) shows the performance of employing various numbers of training and testing samples.

It can be seen from Fig. 8(b) that decreasing the number of training samples leads to increase the EER values. The best EER value has been benchmarked to 0% after using the RPNN by employing a high number of training samples of hand fingers for each individual. By decreasing this number to 16 fingers per individual and increasing the number of the testing samples to 8 fingers per individual, this approximately allowed 66% of overall samples to be used in the training phase and about 34% of overall samples to be evaluated in the training phase, a competitive EER value of 3% after

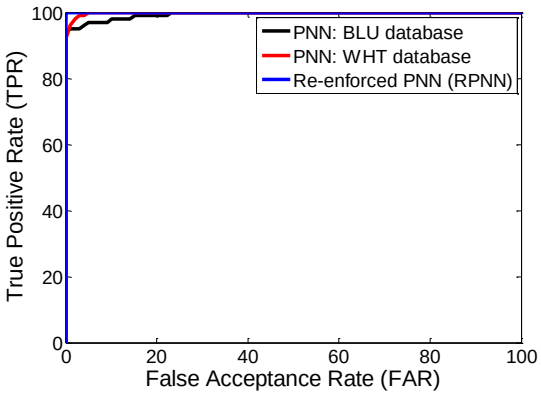

(a)

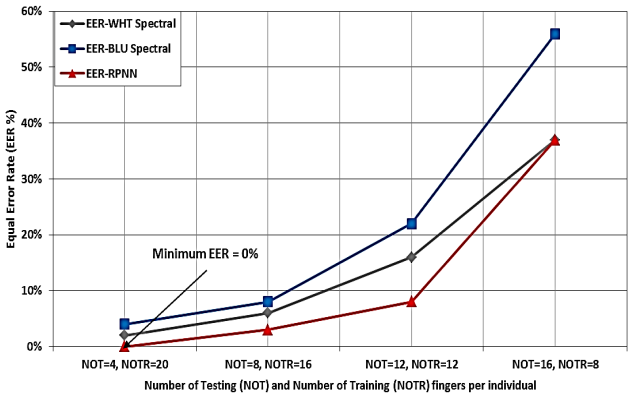

(b)

Fig. 8: Resulted recognition curves:
a ROC curves of the SPC feature extraction for the MSCASIA (WHT), MSCASIA (BLU) and both but by using the RPNN
b EER results after using various numbers of training and testing samples

employing the RPNN has been produced. By decreasing the number of the training samples more the performances of the verification system dramatically reduces. That is, 8% and 37% have been recorded after employing the RPNN when respectively using 50% and approximately 34% of the data in the training phase. Overall, utilizing the RPNN has confirmed its ability to further enhance the EER percentages comparing with separately using the spectra FT images (WHT or BLU).

Moreover, additional evaluation based on the cross-validation has been exploited. The key idea of this method is that the 6 samples of each subject is divided into two subsets: 5 samples for training and 1 sample for testing. This procedure has been implemented 6 times to cover all training and testing subsets. Then, the obtained results have been averaged and the recognition performance has been collected. This method often utilizes for the database that involves few data samples. In this paper, the EER value has been benchmarked to 1.33% by using the cross-validation method. It can be noticed that this EER percentage is still low and this again approves the efficiency of our contributions.

In summary, the advantages of the novel RPNN classifier are as follows:
1. It contains supported information for each subject.
2. It has attained the best verification accuracy of 0% by employing only four fingers. The performance comparisons with publications including the state-of-the-art are given in Table 2.
3. It can be employed with other biometrics which provide multiple inputs. For instance, the iris print images that acquired under two sources of lights: the Near-InfraRed (NIR) and the visible light [35]. In this case for each iris print the two inputs of multi-spectral images can be applied to the RPNN.

6 CONCLUSIONS

This paper has presented a powerful FT verification system based on an effective feature extraction known as the SPC and a novel neural network termed the RPNN. The SPC concentrates on collecting the surrounded patterns around the main FT characteristics, as the best of our knowledge no publication has investigated this matter. This method can efficiently analyse the FT features acquired under two determined lights. The first spectral was for the wavelength of BLU light and the second spectral was for the normal WHT light. Various FT features can be obtained by capturing the finger images under different lighting spectra. Moreover, the RPNN approach was proposed to use the image features of the two spectral lightings by designing a feedback from the output layer to the hidden layer and efficiently managing the trained weights between the main weights and the supported weights. So, it has attractive and powerful architecture. The RPNN has confirmed its capability, flexibility and superiority over the PNN.

It is evident that the SPC method has achieved the best EER values comparing with other feature extraction methods. Furthermore, by applying the RPNN approach to the SPC the EER value has been reduced to 0% and this is the best recorded value in terms of personal verification based on the FT characteristic.

7 Acknowledgements

- The first, second and third authors would like to thank the Ministry of Higher Education and Scientific Research (MOHESR), Iraq.
- Some authors want to give their thanks to: "RC grant EP/P015387/1".
- "The Hong Kong Polytechnic University Contact-free 3D/2D Hand Images Database version 1.0".
- "IIT Delhi Palmprint Image Database version 1.0".
- "Portions of the research in this paper use the CASIA-MS-PalmprintV1 collected by the Chinese Academy of Sciences' Institute of Automation (CASIA)".

8 References

[1] Darwish, S.: 'New system to fingerprint extensible markup language documents using winnowing theory', IET Signal Process., 2012, 6, (4), pp. 348-357

[2] Tan, C., Kumar, A.: 'Accurate Iris Recognition at a Distance Using Stabilized Iris Encoding and Zernike Moments Phase Features', IEEE Trans. on Image Process., 2014, 23, (9), pp. 3962-3974

[3] Zhang, Y., Peng, H.:'One sample per person face recognition via sparse representation', IET Signal Process., 2016, 10, (9), pp. 1126-1134

[4] Štruc, V., Pavešić, N.: 'Phase congruency features for palmprint verification', IET Signal Process., 2009, 3, (4), pp. 258-268

[5] Al-Kaltakchi, M. T. S., Woo, W. L., Dlay, S. S., *et al.*: 'Study of statistical robust closed set speaker identification with feature and score-based fusion'. IEEE Statistical Signal Process Workshop (SSP), 2016, pp. 1-5

[6] Al-Nima, R.R.O., Dlay, S.S., Woo, W.L., *et al.*: 'A novel biometric approach to generate ROC curve from the Probabilistic Neural Network'. 24th IEEE Signal Process. and Commun. Appl. Conf. (SIU), 2016, pp. 141-144

[7] Al-Nima, R.R.O., Dlay, S.S., Woo, W.L.: 'A New Approach to Predicting Physical Biometrics from Behavioural Biometrics', World Academy of Sci., Eng. and Technol., Int. J. of Comput., Electr., Autom., Control and Inf. Eng., 2014, 8, (11), pp. 1996-2001

[8] Bhaskar, B., Veluchamy, S.: 'Hand based multibiometric authentication using local feature extraction'. Int. Conf. Recent Trends Inf. Technol. (ICRTIT), 2014, pp. 1-5

[9] Labati, R.D., Genovese, A., Ballester, E. M., *et al.*: 'Automatic Classification of Acquisition Problems Affecting Fingerprint Images in Automated Border Controls'. IEEE Symposium Series on Comput. Intell., 2015, pp. 354-361

[10] Al-Nima, R.R.O., Dlay, S.S., Al-Sumaidaee, S.A.M., *et al.*: 'Robust feature extraction and salvage schemes for finger texture based biometrics', IET Biometrics, 2017, 6, (2), pp. 43-52

[11] 'CASIA-MS-PalmprintV1', http://biometrics.idealtest.org/, Online Database

[12] Ribaric, S., Fratric, I.: 'A biometric identification system based on eigenpalm and eigenfinger features', IEEE Trans. Pattern Anal. Mach. Intell., 2005, 27, (11), pp. 1698-1709

[13] Pavesic, N., Ribaric, S., Grad, B.: 'Finger-based personal authentication: a comparison of feature-extraction methods based on principal component analysis, most discriminant features and regularised-direct linear discriminant analysis', IET Signal Process., 2009, 3, (4), pp. 269-281

[14] Michael, G.K.O., Connie, T., Jin, A.T.B.: 'Robust palm print and knuckle print recognition system using a contactless approach'. 5th IEEE Conf. Ind. Electron. Appl. (ICIEA), 2010, pp. 323-329

[15] Michael, G.K.O., Connie, T., Jin, A.T.B.: 'An innovative contactless palm print and knuckle print recognition system', Pattern Recognition Lett., 2010, 31, (12), pp. 1708-1719

[16] Kanhangad, V., Kumar, A., Zhang, D.: 'A Unified Framework for Contactless Hand Verification', IEEE Trans. Inf. Forensics Security, 2011, 6, (3), pp. 1014-1027

[17] 'The Hong Kong Polytechnic University Contact-free 3D/2D Hand Images Database version 1.0', http://www.comp.polyu.edu.hk/ csajaykr/myhome/ database_request/3dhand/Hand3D.htm, Online Database

[18] Zhang, Y., Sun, D., Qiu, Z.: 'Hand-based single sample biometrics recognition', Springer, Neural Comput. and Appl., 2012, 21, (8), pp. 1835-1844

[19] Sankaran, A., Malhotra, A., Mittal, A., *et al.*: 'On smartphone camera based fingerphoto authentication'. IEEE 7th Int. Conf. on Biometrics Theory, Appl. and Syst. (BTAS), 2015, pp. 1-7

[20] Al-Nima, R.R.O., Dlay, S.S., Woo, W.L., *et al.*: 'Human Authentication With Finger Textures Based on Image Feature Enhancement'. The 2nd IET Int. Conf. Intell. Signal Process. (ISP), 2015

[21] Al-Nima, R.R.O., Dlay, S.S., Woo, W.L., et al.: 'Efficient finger segmentation robust to hand alignment in imaging with application to human verification'. 5th IEEE Int. Workshop on Biometrics and Forensics (IWBF), 2017, pp. 1-6

[22] Al-Nima, R.R.O., Abdullah, M.A.M., Al-Kaltakchi, M.T.S., *et al.*: 'Finger texture biometric verification exploiting multi-scale sobel angles local binary pattern features and score-based fusion', Elsevier, Digit. Signal Process., 2017, 70, pp. 178-189

[23] Al-Sumaidaee, S.A.M., Abdullah, M.A.M., Al-Nima, R.R.O., *et al.*: 'Multi-gradient features and elongated quinary pattern encoding for image-based facial expression recognition', Elsevier, Pattern Recognition, 2017, 71, pp. 249-263

[24] Raghavendra, R., Busch, C.: 'Novel image fusion scheme based on dependency measure for robust multispectral palmprint recognition', Elsevier, Pattern recognition, 2014, 47, (6), pp. 2205-2221

[25] Junli, L., Gengyun, Y., Guanghui, Z.: 'Evaluation of tobacco mixing uniformity based on chemical composition'. 31st Chinese Control Conf. (CCC), 2012, pp. 7552-7555

[26] Kou, J., Xiong, S., Wan, S., *et al.*: 'The Incremental Probabilistic Neural Network'. 6th Int. Conf. on Natural Comput. (ICNC), 2010, 3, pp. 1330-1333

[27] Khan, Z., Mian, A., Hu, Y.: 'Contour Code: Robust and efficient multispectral palmprint encoding for human recognition'. IEEE Int. Conf. Comput. Vision (ICCV), 2011, pp. 1935-1942

[28] Khan, Zohaib, Shafait, Faisal, Hu, Yiqun, *et al.*: 'Multispectral palmprint encoding and recognition', arXiv preprint arXiv:1402.2941, 2014

[29] Fu, X., Wei, W.: 'Centralized binary patterns embedded with image euclidean distance for facial expression recognition'. 4th Int. Conf. on Natural Comput., 2008, 4, pp. 115-119

[30] Tong, Y., Chen, R., Cheng, Y.: 'Facial expression recognition algorithm using LGC based on horizontal and diagonal prior principle', Elsevier, Optik-Int. J. for Light and Electron Optics, 2014, 125, (16), pp. 4186-4189

[31] Wolf, L., Hassner, T., Taigman, Y.: 'Descriptor based methods in the wild'. Workshop on Faces in 'Real-Life' Images: Detection, Alignment, and Recognition, 2008

[32] Tao, Q., Veldhuis, R.: 'Illumination Normalization Based on Simplified Local Binary Patterns for A Face Verification System'. Biometrics Symposium, 2007, pp. 1-6

[33] 'IIT Delhi Palmprint Image Database version 1.0', http://www4.comp.polyu.edu.hk/ csajaykr/IITD/Database_Palm.htm, Online Database

[34] Kumar, Ajay: 'Incorporating cohort information for reliable palmprint authentication'. 6th IEEE Indian Conf. on Comput. Vision, Graphics & Image Process., ICVGIP'08., 2008, pp. 583-590

[35] Abdullah, M.A.M., Al-Nima, R.R.O., Dlay, S.S., *et al.*: 'Cross-Spectral Iris Matching for Surveillance Applications', In: Karampelas, P., Bourlai, T. (eds): 'Surveillance in Action' (Adv. Sciences and Technologies for Security Appl., Springer, Cham, 2018), pp. 105-125